Quantum repeaters based on trapped ions with decoherence free subspace encoding

M. Zwerger[1], B. P. Lanyon[2,3], T. E. Northup[2], C. A. Muschik[3,4], W. Dür[4], and N. Sangouard[1]
[1] *Departement Physik, Universität Basel, Klingelbergstraße 82, 4056 Basel, Switzerland*
[2] *Institut für Experimentalphysik, Universität Innsbruck, Technikerstraße 25, A-6020 Innsbruck, Austria*
[3] *Institut für Quantenoptik und Quanteninformation der Österreichischen Akademie der Wissenschaften, A-6020 Innsbruck, Austria*
[4] *Institut für Theoretische Physik, Universität Innsbruck, Technikerstraße 21a, A-6020 Innsbruck, Austria*
(Dated: November 24, 2016)

Quantum repeaters provide an efficient solution to distribute Bell pairs over arbitrarily long distances. While scalable architectures are demanding regarding the number of qubits that need to be controlled, here we present a quantum repeater scheme aiming to extend the range of present day quantum communications that could be implemented in the near future with trapped ions in cavities. We focus on an architecture where ion-photon entangled states are created locally and subsequently processed with linear optics to create elementary links of ion-ion entangled states. These links are then used to distribute entangled pairs over long distances using successive entanglement swapping operations performed deterministically using ion-ion gates. We show how this architecture can be implemented while encoding the qubits in a decoherence free subspace to protect them against collective dephasing. This results in a protocol that can be used to violate a Bell inequality over distances of about 800 km assuming state of the art parameters. We discuss how this could be improved to several thousand kilometers in future setups.

arXiv:1611.07779v1 [quant-ph] 23 Nov 2016

I. INTRODUCTION

The ability to establish entanglement over long distances is crucial for applications like quantum key distribution [1–3], distributed quantum computation [4–6], and more generally, quantum networks [7]. In establishing long-distance entanglement, the main difficulties to overcome are loss of qubits and decoherence. Due to the no-cloning theorem [8] one cannot use redundant encoding or amplification as in the classical case. Quantum repeater protocols for scalable communication circumvent these problems by making use of either quantum error correction [9] or entanglement purification and swapping [10] (or combinations thereof). In the first case [9] one encodes quantum information in a quantum error correcting code, sends it through the channel and applies quantum error correction at properly spaced quantum repeater stations. In the second case [10], one first creates entanglement between neighboring repeater stations and then iteratively applies entanglement swapping and purification. Both schemes require the control of a number of qubits at each node which is above what can be handled with present day technology [10–12].

This requirement motivated people to study simpler quantum repeaters without entanglement purification which are not scalable [13], but might beat the direct transmission of photons through fibers. These architectures use a reduced number of qubits and a few entanglement swapping operations so that the errors are small enough to allow quantum communication without entanglement purification. Notice that the term quantum repeater originally referred to scalable protocols but is now commonly used for any long-range quantum communication scheme. Many proposals are based on atomic ensembles and linear optics following the initial work of [14]; for a review see [15]. In [16] a scheme based on single trapped ions was put forward which achieved higher rates than with atomic ensembles, mostly due to deterministic entanglement swapping operations in this setup (see also [17, 18]).

Here we study this approach under the influence of noise and for parameters from the present ion trap setup in Innsbruck. Our figure of merit is the fidelity of the Bell pairs between repeater end nodes, which we require to be large to enough to violate a Bell inequality. This is relevant for device-independent quantum key distribution (QKD) [19]. We find that the scheme proposed in [16] does not allow one to beat direct transmission when taking current collective dephasing within the ion trap into account. We then propose a modified protocol where qubits are encoded in a decoherence free subspace (DFS) [20, 21], which is unaffected by collective dephasing, and show how the encoding and processing of logical Bell states can be done. Such a quantum repeater allows one to reach a distance of around 800 km between repeater end-nodes assuming state of the art parameters.

The outline of the paper is as follows. In Sec. II we describe the system and present the relevant parameters. In Sec. III A and Sec. III B we investigate the fidelities without and with a DFS, respectively. Sec. IV is devoted to the distribution times. In Sec. V we outline how one could reach longer distances by either assuming higher fidelity operations or using logical entanglement purification, before we conclude in Sec. VI.

II. PROTOCOL AND SYSTEM

In this section we describe the direct transmission of quantum information through optical fibers, the quantum repeater protocol which we propose and the system which we are looking at, including the relevant noise processes and parameters.

A. Direct transmission

The direct transmission of quantum information is done by sending an entangled pair of photons at telecom wavelength (1550 nm) through an optical fiber. For short distances, noise can be neglected and the maximum reachable distance is limited by the (expected) time it

takes a photon to arrive at the final destination. For a standard optical fiber the attenuation length is $L_{att} = 22$ km, the speed of light in fiber is $c = 2 \cdot 10^8$ m/s and the transmission probability is $\eta_t = e^{-L_0/L_{att}}$, where L_0 is the total length. We assume a detector efficiency of $\eta_d = 0.9$ [22, 23] and a photon pair creation rate of 10 GHz, corresponding to state-of-the-art generation rates of entangled photons via parametric down conversion. One then finds that one can reach a distance of around 500 km with an average distribution time of around one second (see also Fig. 5). Note that this protocol does not allow one to perform device-independent QKD due to its probabilistic nature.

B. Proposed quantum repeater protocol

The quantum repeater protocol which we propose here can be seen as an extension of [16]. In [16] entanglement is created between trapped ions in optical cavities and photons, which are sent through the channel. At intermediate locations these photons are measured in the Bell basis via linear optics in order to establish entanglement between neighboring quantum repeater nodes. Entanglement between the outermost quantum repeater nodes is achieved by performing (deterministic) Bell measurements within the ion traps at all intermediate quantum repeater stations.

Here we show how it is possible to encode the qubits into a DFS [20, 21] that protects the quantum information from the effects of collective dephasing, an important source of decoherence in trapped ion systems [24]. In addition we illustrate how the scheme can be extended to a scalable quantum repeater using logical entanglement purification and swapping.

C. System

The physical system which we consider is the cavity quantum electrodynamics (CQED) setup in Innsbruck. It consists of an ion trap inside an optical cavity and allows one to create high fidelity ion-photon entanglement, state mapping between ions and photons, and to perform quantum logic between the trapped ions. For more details on ion-trap quantum networks and the role of cavities, see [25–27]. We use the following parameters:

1. Ion-photon entanglement

Ion-photon entanglement can be created with 99.5% fidelity [28, 29], which leads to ion-ion entanglement with 99% fidelity. The state is assumed to be in Werner form, i.e.

$$\rho = F \left|\phi^+\right\rangle \left\langle\phi^+\right| + \tfrac{1-F}{3} \left(\left|\phi^-\right\rangle \left\langle\phi^-\right| + \left|\psi^+\right\rangle \left\langle\psi^+\right| + \left|\psi^-\right\rangle \left\langle\psi^-\right| \right) \quad (1)$$

which can be enforced via depolarization [30]. $|\phi^\pm\rangle$ and $|\psi^\pm\rangle$ denote the Bell states, i.e.,

$$\left|\phi^\pm\right\rangle = \frac{1}{\sqrt{2}} \left(|0\rangle |0\rangle \pm |1\rangle |1\rangle \right) \quad (2)$$

and

$$\left|\psi^\pm\right\rangle = \frac{1}{\sqrt{2}} \left(|0\rangle |1\rangle \pm |1\rangle |0\rangle \right). \quad (3)$$

2. Fiber

As in [16] and in the direct transmission case above (Sec. II A) we assume an attenuation length $L_{att} = 22$ km for the optical fiber (1550 nm wavelength). The speed of light in the fiber is $c = 2 \cdot 10^8$ m/s and the transmission probability $\eta_t = e^{-L_0/L_{att}}$, where L_0 is the transmission length.

3. Photon detector

For the photon detector efficiency we use a detector efficiency $\eta_d = 0.9$ [22, 23].

4. Probability of an ion emitting a single photon into the cavity output mode

In [28], the probability to generate an ion entangled with a photon and to couple that photon into fiber is 14%, and it is argued that 99% efficiency could be achieved with state-of-the-art mirror losses and the choice of an output mirror with higher transmission. The optical cavity in the Innsbruck setup allows enhanced photon collection from a dipole transition at 854 nm, which has a branching ratio that would otherwise be unfavorable. This wavelength has great potential for efficient frequency conversion to the telecom band, as single-photon frequency conversion from red and near-infrared wavelengths to the telecom bands has been demonstrated with several tens of percent total efficiency, limited largely by passive optical losses [31–33]. Note that we do not consider the detrimental effects of noise introduced by photon conversion: in principle this can be filtered out given the narrowband photons emitted by the cavity-ion photon source.

We thus choose a probability $p = 0.35$ for ion-photon entanglement including photon conversion, and we note that these two processes have not yet been combined in an experimental setup.

5. Noisy operations

We model noisy operations by local depolarizing noise followed by the ideal map. For two-qubit operations we assume 0.5% noise, for single-qubit operations 0.1% noise. The local depolarizing noise (LDN) is described by

$$\mathcal{D}(p_g)\rho = p_g \rho + \frac{1-p_g}{4} \left(\rho + X\rho X + Y\rho Y + Z\rho Z \right) \quad (4)$$

where X, Y, Z are the usual Pauli matrices and $1 - p_g$ quantifies the level of noise. Noisy gates $\hat{U}$ are given by

$\hat{U}\prod_a \mathcal{D}(p_g)^{(a)}\rho$, i.e., single-qubit LDN with error parameter p_g on all involved qubits, followed by the ideal operation described by the superoperator $\hat{U}$ with $\hat{U}\rho = U\rho U^\dagger$, where U is the unitary gate.

6. *Collective dephasing*

Collective dephasing on n qubits is described by the map

$$\rho \to \int_{-\infty}^{\infty} e^{-i\theta\sum_{j=1}^{n} Z_j}\rho e^{i\theta\sum_{j=1}^{n} Z_j} p(\theta)d\theta \qquad (5)$$

with $p(\theta) = \frac{1}{\sqrt{2\pi}\sigma} e^{-\frac{\theta^2}{2\sigma^2}}$ and $\sigma = \frac{T}{\tau}$. Z_j denotes the Pauli Z operator on qubit j, T is the time for which the ions have to be stored and τ is the coherence time, for which we assume $\tau = 10$ ms [24, 29]. Collective dephasing can arise from fluctuations in control fields that couple to quantum systems globally. In ion traps, noise in the amplitude of magnetic fields that couple with equal strength to the closely-spaced ion can cause the ions' qubit transition energies to fluctuate in a correlated manner [24]. In the Innsbruck setup, this effect currently limits the qubit coherence time to around 1 ms, and improvements to 10 ms are expected [29]. Further improvements would entail significant experimental overhead, e.g., ultra-stable magnetic filed sources and an enclosure to shield the experiment from magnetic fields.

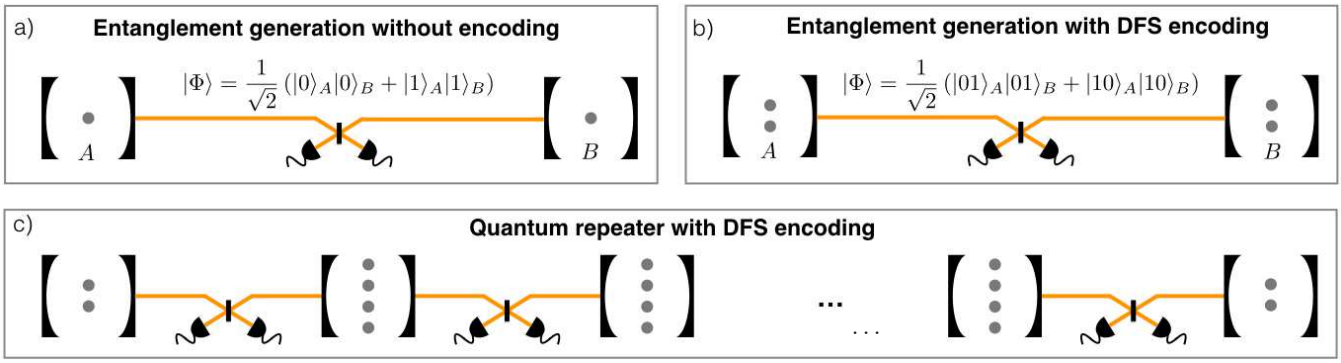


FIG. 1. Illustration of the proposed quantum repeater scheme. At each node ion-photon entanglement is created. The photons are sent to intermediate locations, where a Bell measurement is performed using linear optics (a,b). The resulting Bell pairs between neighboring nodes (cavities) are called links. By performing Bell measurements on the ions at all intermediate nodes, entanglement is swapped over the entire distance (c). Collective dephasing within ion-traps [24] is an important noise mechanism, which severely limits the achievable performance of such quantum repeaters without encoding (see panel a). This problem is mitigated by encoding quantum information in a decoherence free subspace (DFS), $|0\rangle \to |01\rangle$, $|1\rangle \to |10\rangle$, which renders the entangled links insensitive to collective dephasing. The connection of entangled links requires Bell measurements on the logical states, which can be achieved as described in Sec. III B 2.

III. FIDELITIES

In this section we investigate the achievable fidelities for a trapped-ion-based quantum repeater, both when not using and when using a DFS.

A. Quantum repeater based on trapped ions without DFS

Here we study the original proposal [16] in the presence of noise. We assume the parameters given in Sec. II. For the average distribution time for a Bell pair we use the formula [16]

$$T_{tot} \approx \left(\frac{3}{2}\right)^n \frac{L_0}{c}\frac{1}{p^2\eta_t^2\eta_d^2}, \qquad (6)$$

for a quantum repeater with 2^n links. Here, $\frac{L_0}{c}\frac{1}{p^2\eta_t^2\eta_d^2}$ is the expected time it takes to establish a Bell pair within one link, and the factor $\left(\frac{3}{2}\right)^n$ arises from the fact that the entanglement generation needs to be successful in all 2^n links. For more details see [16].

The resulting fidelities for ion-ion entanglement with respect to a maximally entangled state for four, eight, and 16 links are shown as a function of distance in Fig. 2. The offset at zero distance is a result of the imperfect operations and non-unit fidelity of the Bell pairs in the elementary links. The drop as a function of distance is due to the fact that it takes longer to distribute a Bell pair over a longer distance, which means that the ions in each trap are exposed to collective dephasing for a longer time. The fidelity drops below 78%, which is the threshold required to violate a Bell inequality [34, 35], before reaching 20 km. Given the fact that the direct transmission of photons allows one to reach distances of around 500 km (see Fig. 5) we conclude that a quantum repeater based on this architecture (and the noise parameters stated above) will not outperform the direct transmission of (telecom wavelength) photons through fibers.

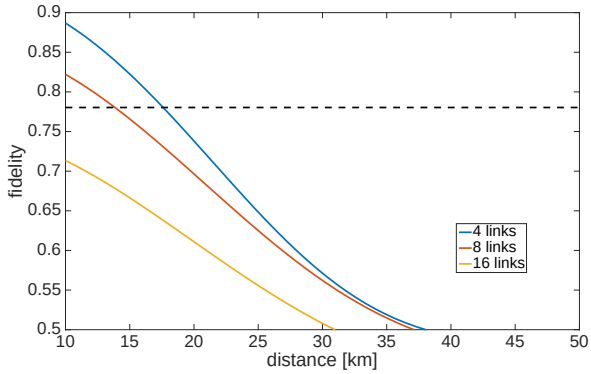


FIG. 2. Performance of a trapped-ion-based quantum repeater without a DFS. The fidelity is plotted as a function of distance for four, eight, and 16 links. In all cases it drops below 78% (dashed line) before reaching 20 km, which implies that it does not outperform the direct transmission of photons. For more details see the main text.

B. Quantum repeater based on trapped ions with DFS

In the previous subsection we have seen that (current) collective dephasing prevents us from beating direct transmission. The effect of collective dephasing can be compensated for by encoding the qubits in a DFS which is invariant under the noise. Notice that using the DFS is a passive form of protection. Unlike quantum error correction it does not require one to measure stabilizer operators and to perform subsequent operations conditioned on the outcomes of these measurements. Thus using the DFS only requires twice as many qubits (as compared to the case without a DFS), performing the encoding and logical swap operations instead of physical ones.

1. *Encoding*

The DFS which is invariant under collective dephasing is spanned by $|0_L\rangle = |01\rangle$ and $|1_L\rangle = |10\rangle$. An unknown state $|\psi\rangle = \alpha\,|0\rangle + \beta\,|1\rangle$ can be encoded by using an ancilla qubit in state $|1\rangle$ and applying a $CNOT$ gate with the ancilla qubit as target. The encoded state is then given by $|\psi_L\rangle = \alpha\,|01\rangle + \beta\,|10\rangle$.

2. *Logical entanglement swap operation*

The swapping of logical entanglement is performed by a logical Bell measurement. There are several possibilities to perform such a logical Bell measurement, two of which are listed below. The first version works probabilistically but allows one to detect errors. The second version is deterministic and includes no error detection.

Version 1 — Here we describe a possibility which requires two entangling gates. Qubits 1 and 3 are on Alice's side, qubits 2 and 4 on Bob's side. The logical Bell measurement is achieved by performing the gates $CNOT^{3\to 2}$ and $CNOT^{1\to 4}$ and then measuring qubits 1 and 3 in the X basis, the other ones in the Z basis. An illustration is given in figure 3. The logical Bell state projection for given results of the single qubit measurements are given in table I. Notice that in the case when one obtains measurement results that are not given in this table (which are all the results that one can obtain as long as the state is in the logical subspace), one discards the resulting state. This corresponds to an error detection scheme and leads to larger fidelities but also makes the protocol probabilistic.

TABLE I. Logical Bell state projection for given results of the single qubit measurements for version 1.

qubit 1	qubit 2	qubit 3	qubit 4	Bell state
+	−	+	−	$\|\phi_L^+\rangle$
−	−	−	−	$\|\phi_L^+\rangle$
+	−	−	−	$\|\phi_L^-\rangle$
−	−	+	−	$\|\phi_L^-\rangle$
+	+	+	+	$\|\psi_L^+\rangle$
−	+	−	+	$\|\psi_L^+\rangle$
+	+	−	+	$\|\psi_L^-\rangle$
−	+	+	+	$\|\psi_L^-\rangle$

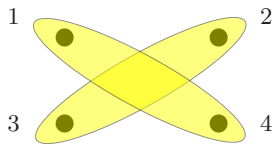


FIG. 3. Illustration of version 1 for a logical Bell measurement. The black dots represent the physical qubits. They are all in the same ion trap. Qubits 1 and 3 are part of one logical Bell pair, qubits 2 and 4 are part of the other logical Bell pair. Only entangling gates are shown (yellow ellipses).

Version 2 — A version which requires only one entangling gate is given by the following protocol (the qubit labeling is the same as above): perform $CNOT^{3\to 4}$ and measure qubits 1, 2 and 3 in the X basis, and qubit 4 in the Z basis. An illustration is given in figure 4. The logical Bell state projection for given results of the single qubit measurements are given in table II.

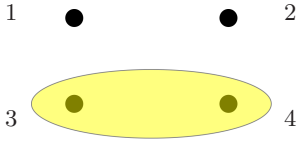


FIG. 4. Illustration of version 2 for a logical Bell measurement. The black dots represent the physical qubits. They are all in the same ion trap. Qubits 1 and 3 are part of one logical Bell pair, qubits 2 and 4 are part of the other logical Bell pair. Only entangling gates are shown (yellow ellipses).

3. *Resulting fidelities*

We compared the fidelities for various numbers of links using the different protocols described above. The version which uses error detection, version 1, performs better than version 2. The fidelities for the case when using version 1 are summarized in table III, the ones for version 2

TABLE II. Logical Bell state projection for given results of the single qubit measurements for version 2.

qubit 1	qubit 2	qubit 3	qubit 4	Bell state
+	+	+	+	$\left\|\phi_L^+\right\rangle$
+	−	−	+	$\left\|\phi_L^+\right\rangle$
−	+	−	+	$\left\|\phi_L^+\right\rangle$
−	−	+	+	$\left\|\phi_L^+\right\rangle$
+	+	−	+	$\left\|\phi_L^-\right\rangle$
+	−	+	+	$\left\|\phi_L^-\right\rangle$
−	+	−	+	$\left\|\phi_L^-\right\rangle$
−	−	+	+	$\left\|\phi_L^-\right\rangle$
+	+	+	−	$\left\|\psi_L^+\right\rangle$
+	−	−	−	$\left\|\psi_L^+\right\rangle$
−	+	−	−	$\left\|\psi_L^+\right\rangle$
−	−	+	−	$\left\|\psi_L^+\right\rangle$
+	+	−	−	$\left\|\psi_L^-\right\rangle$
+	−	+	−	$\left\|\psi_L^-\right\rangle$
−	+	+	−	$\left\|\psi_L^-\right\rangle$
−	−	−	−	$\left\|\psi_L^-\right\rangle$

TABLE III. Fidelities for different numbers of links when using version 1. The maximal number of links such that the fidelity is still large enough to violate a Bell inequality is given by 10.

# links	4	8	10	11
fidelity	90.1%	82.3%	78.7%	77.0%

in table IV. These are the fidelities of the Bell pairs after the decoding, which is simply the inverse of the encoding circuit described above. There is a slight drop of the fidelity as a function of distance, despite the fact that the logical qubits are unaffected by collective dephasing due to the DFS. We attribute this to the imperfect (noisy) encoding, which leads to populations outside the logical subspace. Empirically we find that this drop is at most of the order of 0.5% between distance zero and the distance which corresponds to a distribution time of a second. The fidelities which we present here are evaluated at a distance which corresponds to a distribution time of (at least) a second and thus represent a lower bound. The maximally reachable distance is limited by the distribution time (see Sec. IV). We analyzed the density matrices of the Bell pairs and found that they are diagonal in the Bell basis. Using depolarization [30] one can bring them into Werner state form and thus describe them by

$$\rho = \mathcal{D}_1(\tilde{p})\mathcal{D}_2(\tilde{p}) \left|\phi^+\right\rangle \left\langle\phi^+\right| . \tag{7}$$

In order to violate a Bell inequality [34, 35] the fidelity needs to exceed 78.0%. This minimum fidelity puts a constraint on the maximum number of repeater links and thus on the maximally reachable distance for fixed distribution time.

TABLE IV. Fidelities for different numbers of links when using version 2. The maximal number of links such that the fidelity is still large enough to violate a Bell inequality is given by 7.

# links	4	6	7	8
fidelity	87.4%	81.9%	79.4%	76.9%

IV. DISTRIBUTION TIMES

The time it takes to establish an entangled pair is given by the time until there is entanglement in all links. The entanglement waiting times in each segment are (independent) geometrically distributed random variables. Using the fact that the minimum of n identical geometric random variables with success probability p is itself geometric with success probability $1-(1-p)^n$ (see also [36]) one obtains for the (expected) distribution time T

$$T = \frac{L_0}{c} \sum_{n=1}^{N} \frac{1}{1-(1-P_{link})^n} \tag{8}$$

where P_{link} is the success probability for creating entanglement in a single link, i.e. $P_{link} = \frac{1}{2p^2\eta_t^2\eta_d^2}$, and N is the total number of links.

The time for the classical communication (the measurement results from the logical Bell measurements need to be communicated) is bounded from above by $\frac{NL_0}{c}$.

When one uses version 1 for logical entanglement swapping one has to repeat the entanglement distribution on average P^{-1} times, where P is the probability that one obtains successful outcomes (i.e., the ones in table I) for all entanglement swaps.

The resulting distribution times are shown in Fig. 5, where the direct transmission of a photon pair with a pair creation rate of 10 GHz is added for comparison. The parameters are those stated in Sec. II.

We see that one can reach the largest distance, approximately 800 km, for a fixed distribution time of one second with version 1 for the logical entanglement swapping.

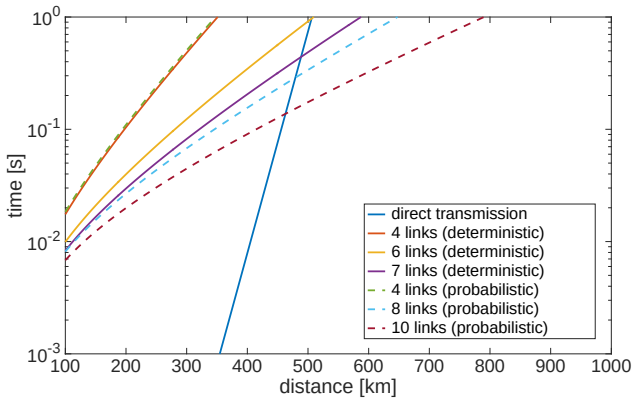


FIG. 5. Distribution time for various numbers of links and both versions for entanglement swapping and direct transmission for comparison. We assumed the following parameters: photon detector efficiency $\eta_d = 0.9$, probability of ion emitting a single photon $p = 0.35$, fiber attenuation length $L_{att} = 22$ km and speed of light in fiber $c = 2{\cdot}10^8$ m/s. For the direct transmission we assumed a pair creation rate of 10 GHz.

V. ACHIEVING LONGER DISTANCES

There are different strategies which would allow us to reach longer distances. Two possibilities are sketched below, both of which require more advanced technology.

A. Higher fidelity operations

One possibility is to increase the fidelity of the ion-photon entanglement and the gates. The resulting fidelities, when assuming ion-ion entanglement with 99.9% fidelity and single-(two) qubit gates with 0.01 (0.1)% noise, are provided in tables V and VI for version 1 and 2 of the swapping operations, respectively. The assumed noise parameters are beyond what has been demonstrated in the current setup, but it should be noted that gates with such low noise have already been achieved in other ion trap setups [37].

The corresponding distribution times are plotted in Fig. 6, assuming that the probability of an ion emitting a single photon followed by successful frequency conversion is given by $p = 0.75$. Ion-cavity setups and photon conversion devices are not available now with these efficiencies, but such probabilities are reasonable assuming state-of-the-art cavities and the fact that there is no fundamental limit to photon conversion efficiency

In summary, we see that the quantum repeater based on trapped ions and using a DFS as described above is capable of extending quantum communication to distances of several thousand kilometers assuming futuristic but reasonable parameters.

TABLE V. Fidelities for different numbers of links when assuming that the fidelity of ion-ion entanglement is given by 99.9% and 0.01 (0.1)% noise for single-(two) qubit gates. Here we use version 1 for the logical entanglement swapping.

# links	16	32	64	70	71	72
fidelity	96.9%	89.0%	79.9%	78.3%	78.1%	77.8%

TABLE VI. Fidelities for different numbers of links when assuming that the fidelity of ion-ion entanglement is given by 99.9% and 0.01 (0.1)% noise for single-(two) qubit gates. Here we use version 2 for the logical entanglement swapping.

# links	16	32	47	48
fidelity	91.7%	84.4%	78.2%	77.9%

B. Full quantum repeater with entanglement purification and DFS encoding

A second possibility to increase the maximally reachable distance is to include entanglement purification, so that the scheme becomes scalable [10]. The idea is the following: the Bell pairs in each link are encoded into a DFS in order to protect them from collective dephasing. Subsequently one performs entanglement purification and swapping of logical Bell pairs in a nested way

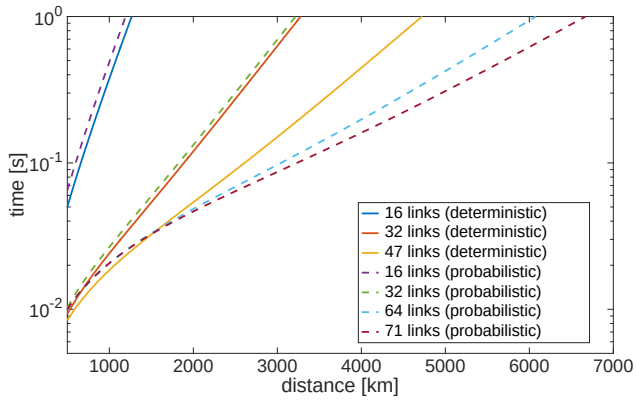


FIG. 6. Distribution time for various numbers of links and both versions of entanglement swapping assuming that the probability of an ion emitting a single photon followed by successful frequency conversion is $p = 0.75$. The other parameters are: photon detector efficiency $\eta_d = 0.9$, fiber attenuation length $L_{att} = 22$ km and speed of light in fiber $c = 2 \cdot 10^8$ m/s.

[10]. This requires significantly larger quantum memories at each node [10, 11]. The distribution times are unaffected (compared to the case with no entanglement purification) as long as one uses a one-way entanglement purification protocol (see [38] for a discussion on the role of memory errors in quantum repeater schemes using one-way and two-way communication in entanglement purification).

In order to implement purification one needs to be able to perform Clifford gates and Pauli measurements. Below we provide a set of generators of logical Clifford gates (qubits 1 and 2 (3 and 4) encode the first (second) logical qubit) for the encoding $|0_L\rangle = |01\rangle$ and $|1_L\rangle = |10\rangle$:

$$\begin{aligned} S_L &= S^1 \\ H_L &= [(HSHZ) \otimes (HSH)]\, CNOT^{1\to 2}\, [(HSX) \otimes X] \\ CZ_L &= CZ^{1\to 3}, \end{aligned} \tag{9}$$

where $S = \mathrm{diag}(1, i)$ (in the computational basis) is a rotation around the Z-axis by an angle $\frac{\pi}{2}$, H is the Hadamard gate and $CZ = \mathrm{diag}(1, 1, 1, -1)$ denotes the controlled phase gate. A measurement in the logical computational basis can be performed by measuring the first physical qubit in the computational basis. Notice that any Clifford circuit can be realized by combining these generating operations. However, for particular protocols a direct implementation of the required logical unitary operation using fewer two-qubit gates might be possible.

This allows one to implement one-way and two-way entanglement purification protocols at the logical level. In particular, one can implement the recurrence protocol of [39] that is used in the scalable repeater scheme of [10]. In this case, entanglement between logical states is established between neighboring nodes, where two (or more) basic links are connected. The DFS encoding protects the system against memory errors. Before the entanglement drops below a certain threshold value, entanglement purification at the logical level is used to re-establish long-distance pairs with increased fidelity. We remark that also schemes based on error correction, i.e. transmission of encoded information with a DFS encoding at the lowest level, can be implemented in this way when using CSS

codes, as also in this case all required operations are of Clifford type.

VI. CONCLUSIONS

We analyzed the quantum repeater based on trapped ions [16] for realistic parameters for qubit coherence, logic gate operations, ion-photon entanglement, and photon collection and detection efficiencies. We have found that the repeater's performance is severely limited by collective dephasing within the ion traps. We then proposed a modified protocol where the qubits are encoded in a decoherence free subspace and showed that this allows one to reach distances of approximately 800 km for state of the art parameters. By considering parameters that have not been achieved yet, but can realistically be expected to be obtainable in the trapped-ion platform, we found that the reachable distance can be extended by almost an order of magnitude to several thousand kilometers. This allows one to reach intercontinental distances, even without entanglement purification, with fidelities that are even high enough to violate Bell inequalities. In future work, it will be important to extend our analysis to include the limitations imposed by other sources of error, e.g., photon indistinguishability.

The usage of a decoherence free subspace as a lowest layer of protection against dominant noise sources is not restricted to ion trap set-ups. One can use a similar approach in other systems, e.g. NV-centers (see [40]). Finally, we remark that higher rates can in principle be reached using an approach based on the transmission of encoded information (see [9, 41, 42]). However, this comes at the price of a large overhead in required resources, on the one hand due to small repeater spacing (of the order of 1 km) and on the other hand due to the large number of ions to be processed at each node because one uses a (concatenated) error correction code. To compare the performance and resource requirements of such a scheme to our approach for the same set-up would be interesting.

ACKNOWLEDGEMENTS

This work was supported by the Swiss National Science Foundation (SNSF) through Grant number PP00P2-150579, the Army Research Laboratory Center for Distributed Quantum Information via the project SciNet, the EU via the integrated project SIQS, and the Austrian Science Fund (FWF): P28000 - N27.

[1] C. H. Bennett and G. Brassard, in *Proceedings of IEEE International Conference on Computers, Systems and Signal Processing* (IEEE Computer Society, Bangalore, India, 1984) pp. 175–179.
[2] A. K. Ekert, Phys. Rev. Lett. **67**, 661 (1991).
[3] V. Scarani, H. Bechmann-Pasquinucci, N. J. Cerf, M. Dušek, N. Lütkenhaus, and M. Peev, Rev. Mod. Phys. **81**, 1301 (2009).
[4] R. V. Meter and M. Oskin, J. Emerg. Technol. Comput. Syst. **2**, 31 (2006).
[5] R. V. Meter, W. J. Munro, K. Nemoto, and K. M. Itoh, J. Emerg. Technol. Comput. Syst. **3**, 2:1 (2008).
[6] R. Beals, S. Brierley, O. Gray, A. W. Harrow, S. Kutin, N. Linden, D. Shepherd, and M. Stather, Proceedings of the Royal Society of London A: Mathematical, Physical and Engineering Sciences **469** (2013).
[7] H. J. Kimble, Nature **453**, 1023 (2008).
[8] W. Wootters and W. Zurek, Nature **299**, 802 (1982).
[9] E. Knill and R. Laflamme, "Concatenated Quantum Codes," (1996), arXiv:quant-ph/9608012.
[10] H.-J. Briegel, W. Dür, J. I. Cirac, and P. Zoller, Phys. Rev. Lett. **81**, 5932 (1998).
[11] W. Dür, H.-J. Briegel, J. I. Cirac, and P. Zoller, Phys. Rev. A **59**, 169 (1999).
[12] S. Muralidharan, L. Li, J. Kim, N. Lütkenhaus, M. D. Lukin, and L. Jiang, Scientific Reports **6**, 20463 EP (2016).
[13] A quantum repeater is scalable if one can create a Bell pair with a fidelity exceeding a predefined value over arbitrarily long distances with at most polynomially growing resources.
[14] L. M. Duan, M. D. Lukin, J. I. Cirac, and P. Zoller, Nature **414**, 413 (2001).
[15] N. Sangouard, C. Simon, H. de Riedmatten, and N. Gisin, Rev. Mod. Phys. **83**, 33 (2011).
[16] N. Sangouard, R. Dubessy, and C. Simon, Phys. Rev. A **79**, 042340 (2009).
[17] L.-M. Duan and C. Monroe, Rev. Mod. Phys. **82**, 1209 (2010).
[18] A. D. Pfister, M. Salz, M. Hettrich, U. G. Poschinger, and F. Schmidt-Kaler, Applied Physics B **122**, 89 (2016).
[19] N. Brunner, D. Cavalcanti, S. Pironio, V. Scarani, and S. Wehner, Rev. Mod. Phys. **86**, 419 (2014).
[20] P. Zanardi and M. Rasetti, Phys. Rev. Lett. **79**, 3306 (1997).
[21] D. A. Lidar, I. L. Chuang, and K. B. Whaley, Phys. Rev. Lett. **81**, 2594 (1998).
[22] A. E. Lita, A. J. Miller, and S. W. Nam, Opt. Express **16**, 3032 (2008).
[23] F. Marsili, V. B. Verma, J. A. Stern, S. Harrington, A. E. Lita, T. Gerrits, I. Vayshenker, B. Baek, M. D. Shaw, R. P. Mirin, and S. W. Nam, Nat Photon **7**, 210 (2013).
[24] T. Monz, P. Schindler, J. T. Barreiro, M. Chwalla, D. Nigg, W. A. Coish, M. Harlander, W. Hänsel, M. Hennrich, and R. Blatt, Phys. Rev. Lett. **106**, 130506 (2011).
[25] T. E. Northup and R. Blatt, Nat Photon **8**, 356 (2014).
[26] L.-M. Duan and C. Monroe, Rev. Mod. Phys. **82**, 1209 (2010).
[27] A. Stute, B. Casabone, B. Brandstätter, D. Habicher, H. G. Barros, P. O. Schmidt, T. E. Northup, and R. Blatt, Applied Physics B **107**, 1145 (2012).
[28] A. Stute, B. Casabone, P. Schindler, T. Monz, P. O. Schmidt, B. Brandstatter, T. E. Northup, and R. Blatt, Nature **485**, 482 (2012).
[29] P. Schindler, D. Nigg, T. Monz, J. T. Barreiro, E. Martinez, S. X. Wang, S. Quint, M. F. Brandl, V. Nebendahl, C. F. Roos, M. Chwalla, M. Hennrich, and R. Blatt, New Journal of Physics **15**, 123012 (2013).
[30] C. H. Bennett, G. Brassard, S. Popescu, B. Schumacher, J. A. Smolin, and W. K. Wootters, Phys. Rev. Lett. **76**, 722 (1996).

[31] S. Zaske, A. Lenhard, C. A. Keßler, J. Kettler, C. Hepp, C. Arend, R. Albrecht, W.-M. Schulz, M. Jetter, P. Michler, and C. Becher, Phys. Rev. Lett. **109**, 147404 (2012).
[32] B. Albrecht, P. Farrera, X. Fernandez-Gonzalvo, M. Cristiani, and H. de Riedmatten, Nature Communications **5**, 3376 EP (2014).
[33] J. S. Pelc, L. Ma, C. R. Phillips, Q. Zhang, C. Langrock, O. Slattery, X. Tang, and M. M. Fejer, Opt. Express **19**, 21445 (2011).
[34] J. S. Bell, Physics **1**, 195 (1964).
[35] J. F. Clauser, M. A. Horne, A. Shimony, and R. A. Holt, Phys. Rev. Lett. **23**, 880 (1969).
[36] O. A. Collins, S. D. Jenkins, A. Kuzmich, and T. A. B. Kennedy, Phys. Rev. Lett. **98**, 060502 (2007).
[37] C. J. Ballance, T. P. Harty, N. M. Linke, M. A. Sepiol, and D. M. Lucas, Phys. Rev. Lett. **117**, 060504 (2016).
[38] L. Hartmann, B. Kraus, H.-J. Briegel, and W. Dür, Phys. Rev. A **75**, 032310 (2007).
[39] D. Deutsch, A. Ekert, R. Jozsa, C. Macchiavello, S. Popescu, and A. Sanpera, Phys. Rev. Lett. **77**, 2818 (1996).
[40] A. Reiserer, N. Kalb, M. S. Blok, K. J. M. van Bemmelen, T. H. Taminiau, R. Hanson, D. J. Twitchen, and M. Markham, Phys. Rev. X **6**, 021040 (2016).
[41] M. Zwerger, H.-J. Briegel, and W. Dür, Scientific Reports **4**, 5364 (2014).
[42] S. Muralidharan, J. Kim, N. Lütkenhaus, M. D. Lukin, and L. Jiang, Phys. Rev. Lett. **112**, 250501 (2014).